

Research Article

Characteristics of Carbon Monoxide Oxidization in Rich Hydrogen by Mesoporous Silica with TiO₂ Photocatalyst

Akira Nishimura,¹ Yutaka Yamano,¹ Tomokazu Hisada,¹ Masafumi Hirota,¹ and Eric Hu²

¹Division of Mechanical Engineering, Graduate School of Engineering, Mie University, 1577 Kurimamachiya-cho, Tsu 514-8507, Japan

²School of Mechanical Engineering, The University of Adelaide, Adelaide, SA 5005, Australia

Correspondence should be addressed to Akira Nishimura, nisimura@mach.mie-u.ac.jp

Received 17 August 2010; Accepted 9 November 2010

Academic Editor: Jimmy Yu

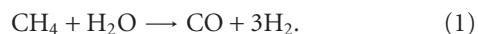
Copyright © 2010 Akira Nishimura et al. This is an open access article distributed under the Creative Commons Attribution License, which permits unrestricted use, distribution, and reproduction in any medium, provided the original work is properly cited.

Hydrogen (H₂) is normally used as the fuel to power polymer electrolyte fuel cell (PEFC). However, the power generation performance of PEFC is harmed by the carbon monoxide (CO) in the H₂ that is often produced from methane (CH₄). The purpose of this study is to investigate the experimental conditions in order to improve the CO oxidization performance of mesoporous silica loaded with TiO₂. The impact of loading ratio of TiO₂ and initial concentration ratio of O₂ to CO on CO oxidization performance is investigated. As a result, the optimum loading ratio of TiO₂ and initial concentration ratio of O₂ to CO were 20 wt% and 4 vol%, respectively, under the experimental conditions. Under this optimum experimental condition, the CO in rich H₂ in the reactor can be completely eliminated from initial 12000 ppmV after UV light illumination of 72 hours.

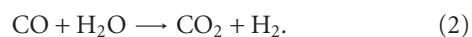
1. Introduction

Polymer electrolyte fuel cell (PEFC) has been developed vigorously in the world since it is an attractive and clean power generation technology. H₂ is normally used as the fuel to power PEFC. However, the reduction of PEFC power generation performance has been observed due to the existence of CO in the H₂ produced from CH₄, CH₃OH, and gasoline.

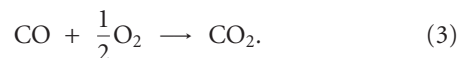
CH₄ is normally the feedstock to produce H₂ with Ni or Ru as catalyst at the high temperature range of 873 K–973 K through the following reaction:



After this reaction, there is about 10 vol% of CO in the products. The CO concentration can be reduced down to about 1 vol% by the following so-called shift reaction:



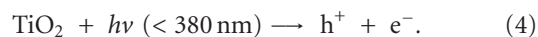
After the shift reaction, the concentration of CO needs to be further reduced down to 10 ppmV by the following selective oxidization reaction:



In the H₂ purification processes mentioned above, precious metal catalysts and thermal energy are used, and the processes are costly. An alternative process, that is, using the TiO₂ photocatalyst combined with adsorbent to oxidize CO is being developed recently due to its potential cost and energy saving.

TiO₂ can oxidize CO under illumination of ultraviolet (UV) ray (available in sunlight) through the following reaction scheme [1, 2].

Photocatalytic reaction:



Oxidization of CO:



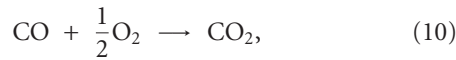
Reduction of O₂:



From the products of the reactions (5) and (8), the following combined reaction occurs:



Therefore, the total reaction scheme can be written as follows:



where $h\nu$ is the energy of UV ray. h^+ and e^- represent the hole and electron produced by photocatalytic reaction, respectively.

The oxidization process with TiO₂ has the following merits. (1) There is a lot of TiO₂ reserve in the earth compared with precious metal catalyst. The amount of Ti is the 9th largest among the elements consisting the earth crust [3]. (2) Cost is lower than using precious metal catalyst. (3) Energy consumption is less and the control of the reaction process is easier since high thermal energy is not necessary. (4) Solar energy can be used for the reaction. (5) TiO₂ is stable in both acid and alkali environments.

Literature survey shows that TiO₂ photocatalyst combined with adsorbent such as activated carbon, zeolite, and silica (SiO₂) was mainly used in environmental purification technologies such as NO_x removal [4–6], decomposition of acetaldehyde [7], dimethylsulfide [8], 2-propanol [9], degradation of organophosphate and phosphoglycine [10], and CO₂ reforming into fuel like CH₄ and CH₃OH [11, 12]. The CO oxidization by photocatalyst combined with FeO_x, Al₂O₃, or CeO_x and precious metal catalyst like Pt or Au was reported [13–15]. Furthermore, the CO oxidization characteristics of Pt loaded on zeolite without photocatalyst were also reported [16, 17]. Although there are reports on the CO oxidization characteristics of Mo/SiO₂ or Cr/SiO₂ [18, 19], there is no report on the CO oxidization characteristics of TiO₂ combined with adsorbent except our previous study [20]. Our previous study investigated the effect of different loading methods of TiO₂ to silica on CO oxidization performance. Comparing two types of TiO₂ particle combined with silica, that is, the silica gel particles coated with TiO₂ film and mesoporous silica particles loaded with TiO₂, the amount of oxidized CO per unit mass of TiO₂ for the mesoporous silica particles loaded with TiO₂ was larger than that for silica gel particles coated with TiO₂ film. Therefore, it revealed that loading was a more effective way to make use of TiO₂ for CO oxidization. However, it also reported that the investigation on optimum experimental condition was necessary to promote the CO oxidization performance more.

The purpose of this study is to investigate the experimental conditions in order to improve the CO oxidization performance of mesoporous silica loaded with TiO₂.

TABLE 1: Physical properties of mesoporous silica loaded with TiO₂.

| | Mesoporous silica loaded with TiO ₂ particles |
|---|---|
| Particle size (mm) | 0.03–0.25 (primary particle) 2.0–5.6 (agglomerated particle) |
| Specific surface area (m ² /g) | 219–1038 |
| Average pore diameter (nm) | 2.7–3.1 |
| Pore volume (mL/g) | 0.63–0.94 |
| Ratio of loaded TiO ₂ (wt%) | 1, 10, 15, 20, 30, 60, 80 |

Since UV ray can penetrate the mesoporous silica, the particles of mesoporous silica loaded with TiO₂ can be used in a bed-type reactor. The effect of loading ratio of TiO₂ and initial concentration ratio of O₂ to CO on CO oxidization performance was investigated to decide the optimum experimental conditions. The loading ratio of TiO₂ is changed minutely by 1 wt%, 10 wt%, 15 wt%, 20 wt%, 30 wt%, 60 wt%, and 80 wt%. The initial concentration of O₂ is also changed closely by 0.5 vol%, 1 vol%, 2 vol%, 4 vol%, 6 vol%, 8 vol%, and 10 vol%. Moreover, the best CO oxidization performance of the mesoporous silica with TiO₂ was evaluated under the optimum experimental conditions.

2. Experiment

2.1. *Preparation Method of Mesoporous Silica Loaded with TiO₂*. Table 1 lists the physical properties of mesoporous silica loaded with TiO₂, which has the following characteristics

- (i) Average pore size is in nanoscale. Since the molecular diameter of CO and O₂ is relatively close to the average pore diameter, the high adsorption performance is expected.
- (ii) TiO₂ particle is located inside of pores of the mesoporous silica. Light can pass through mesoporous silica, and gases can also get into the pores of mesoporous silica through the diffusion, therefore, good photocatalytic reaction as well as good adsorption performance can be expected.

Figure 1 shows the preparation method of mesoporous silica particles loaded with TiO₂ in our laboratory, which is developed by referring to the literatures [21–23]. P25 (Degussa, P25, JAPAN AEROSIL Corp., LTD.) powder was selected as TiO₂ source to load. Because of the primary particle size of P25 which is ranged between 20 nm and 30 nm, P25 is suitable for being inserted into the mesoporous silica particle whose size is ranged between 30 nm and 100 nm generally. P25 plays the role of the core for forming mesoporous silica. The pores of mesoporous silica are formed in or around the particles of P25 as illustrated in Figure 2 [23]. Figure 3 shows TEM image of prepared mesoporous silica particles loaded with TiO₂ to understand the structure illustrated in Figure 2. The ratio of loaded TiO₂ to mesoporous silica was controlled by the amount of P25 added to the mixture solution of ion-exchange water, CH₃(CH₂)₁₅N(CH₃)₃Br (purity of 99 wt%, Nacalai Tesque

Corp.), $(\text{C}_2\text{H}_5\text{O})_4\text{Si}$ (purity of 95 wt%, Nacalai Tesque Corp.), and NH_3 (purity of 28 wt%, Nacalai Tesque Corp.). The amount of P25 particle added to mixture solution was 0.05 g, 0.54 g, 0.86 g, 1.18 g, 2.10 g, 7.30 g, and 19.5 g for the ratio of 1 wt%, 10 wt%, 15 wt%, 20 wt%, 30 wt%, 60 wt%, and 80 wt%, respectively. Here, the ratio of loaded TiO_2 is named after preparation condition since it is very difficult to measure the weight of TiO_2 in mesoporous silica particle directly after preparation process. Particle size of agglomerated mesoporous silica particles loaded with TiO_2 was sieved into the range between 2.0 mm and 5.6 mm after burning.

2.2. Experimental Apparatus and Procedure. Figure 4 illustrates the experimental apparatus which consists of a reactor, a gas mixing chamber, a mass flow controller (MODEL 3660, KOFLOC), a dew point meter (HMT337, VAISALA), a regulator, and a gas cylinder. The reactor, which is a batch type, consists of stainless steel pipe (450 mm (L.) \times 60.5 mm (O.D.) \times 2.5 mm (t.); reaction space 50 mm (L.) \times 55.5 mm (I.D.)) which includes two acrylic cylinders to cover both ends of UV lamp in it, gas supply and exhaust pipe, valves, gas sampling tap, and UV lamp (FL15BLB, TOSHIBA Co., 436 mm (L.) \times 25.5 mm (D.)) located at the center of stainless steel pipe. The reaction space for charging gas and filling TiO_2 particles is $9.22 \times 10^4 \text{ mm}^3$. The central wavelength and mean light intensity of UV light is 352 nm and 4.34 mW/cm^2 , respectively. This light intensity is almost the same as the UV intensity in solar radiation at daytime in the summer of Japan.

In the experiment, O_2 (purity of 99.9999 vol%) and the premixed gas of H_2 and CO (H_2 : 99 vol%, CO: 1 vol%) were mixed in the gas mixing chamber before being supplied to the reactor. By adjusting the flow rate and the pressure of the gases, the initial concentration of O_2 to CO could be controlled. This remixed gas was charged into the reactor, and the concentration and pressure of gases were confirmed before starting the experiment. The ratios of gasses were charged as $\text{CO}:\text{O}_2 = 1:0.5, 1:1, 1:2, 1:4, 1:6, 1:8, \text{ and } 1:10$ (balanced by H_2). Although 1 mol CO reacts with 0.5 mol O_2 theoretically as shown in the reaction of (10), it is necessary to confirm the practical optimum initial concentration ratio of O_2 to CO in rich H_2 environment.

The total pressure in the reactor was set at 0.1 MPa. The gas temperature in the reactor was kept at about 300 K during the experiment. Before the mixed gas for CO oxidization was supplied, mesoporous silica particles loaded with TiO_2 were filled into the reactor by 50 vol% of full reactor volume size.

The experiment was started when illumination of UV light was applied. The gas in reactor was sampled hourly during the experiment. The gas excluding H_2O vapor samples was analyzed by TCD gas chromatograph (VARIAN micro-GC CP-4900, GL Science Corp.) equipped with double columns of Molsieve 5A and PoraPLOT Q. The minimum resolution of the gas chromatograph was 1 ppmV. The concentration of H_2O vapor in the experimental apparatus was measured by the dew point meter whose minimum resolution was 1 ppmV.

3. Results and Discussion

3.1. Effect of Loading Ratio of TiO_2 on CO Oxidization Performance. Figures 5 and 6 show the concentration change of CO_2 and CO with UV light illumination time for the different loading ratios of TiO_2 . From these figures, it can be seen that the concentration of CO for each loading ratio of TiO_2 is decreased with the increase of UV light illumination time, while the concentration of CO_2 is increased. Although the amount of CO reduced does not match the amount of CO_2 produced which is predicted by (9), the reason of it is that the CO adsorption performance of prepared mesoporous silica loaded with TiO_2 is different among different loading ratios. The increase ratio of CO_2 with time is estimated by the following regression line which is derived according to the tendency of data plot:

$$[\text{CO}_2] = R_{\text{inc-CO}_2} t, \quad (11)$$

where $[\text{CO}_2]$ is the concentration of CO_2 at each time (ppmV), $R_{\text{inc-CO}_2}$ stands for the increase ratio of CO_2 (ppmV/h), and t is the time for UV light illumination (h). According to Figure 5, $R_{\text{inc-CO}_2}$ is 159 ppmV/h, 412 ppmV/h, 493 ppmV/h, 706 ppmV/h, 542 ppmV/h, 527 ppmV/h, and 259 ppmV/h for loading ratio of TiO_2 of 1 wt%, 10 wt%, 15 wt%, 20 wt%, 30 wt%, 60 wt%, and 80 wt%, respectively. $R_{\text{inc-CO}_2}$ is larger with the increase in loading ratio of TiO_2 up to 20 wt%, while it becomes smaller with the increase in loading ratio of TiO_2 from 30 wt%. Although the amount of TiO_2 loaded in mesoporous silica is increased with the increase in loading ratio of TiO_2 , which alludes to that the CO oxidization performance is promoted with the increase in the loading ratio of TiO_2 , the optimum loading ratio of TiO_2 is in the middle ratio.

To compare the oxidization rate of CO, Figure 7 shows the change of residual ratio of CO with UV light illumination time for different loading ratios of TiO_2 . The residual ratio of CO is defined as

$$R_{\text{res-CO}} = \frac{[\text{CO}]}{[\text{CO}]_0} \times 100, \quad (12)$$

where $R_{\text{res-CO}}$ stands for the residual ratio of CO (%), $[\text{CO}]$ is the concentration of CO at each time (ppmV), and $[\text{CO}]_0$ is the initial concentration of CO at the beginning of the experiment (ppmV). Regression line is derived according to the tendency of data plot:

$$R_{\text{res-CO}} = 100e^{-\alpha t}, \quad (13)$$

where α is the coefficient of CO removal (1/h). According to Figure 7, the α which indicates the oxidization rate of CO is $9.40 \times 10^{-3}, 8.30 \times 10^{-2}, 1.31 \times 10^{-1}, 1.11 \times 10^{-1}, 1.42 \times 10^{-1}, 9.81 \times 10^{-2}, \text{ and } 2.54 \times 10^{-2}$, for loading ratio of TiO_2 of 1 wt%, 10 wt%, 15 wt%, 20 wt%, 30 wt%, 60 wt% and 80 wt%, respectively. α is larger with the increase in loading ratio of TiO_2 up to 30 wt%, after that, it is smaller with the increase in loading ratio of TiO_2 .

Figure 8 shows the comparison of selection ratio of CO oxidization among different loading ratios of TiO_2 .

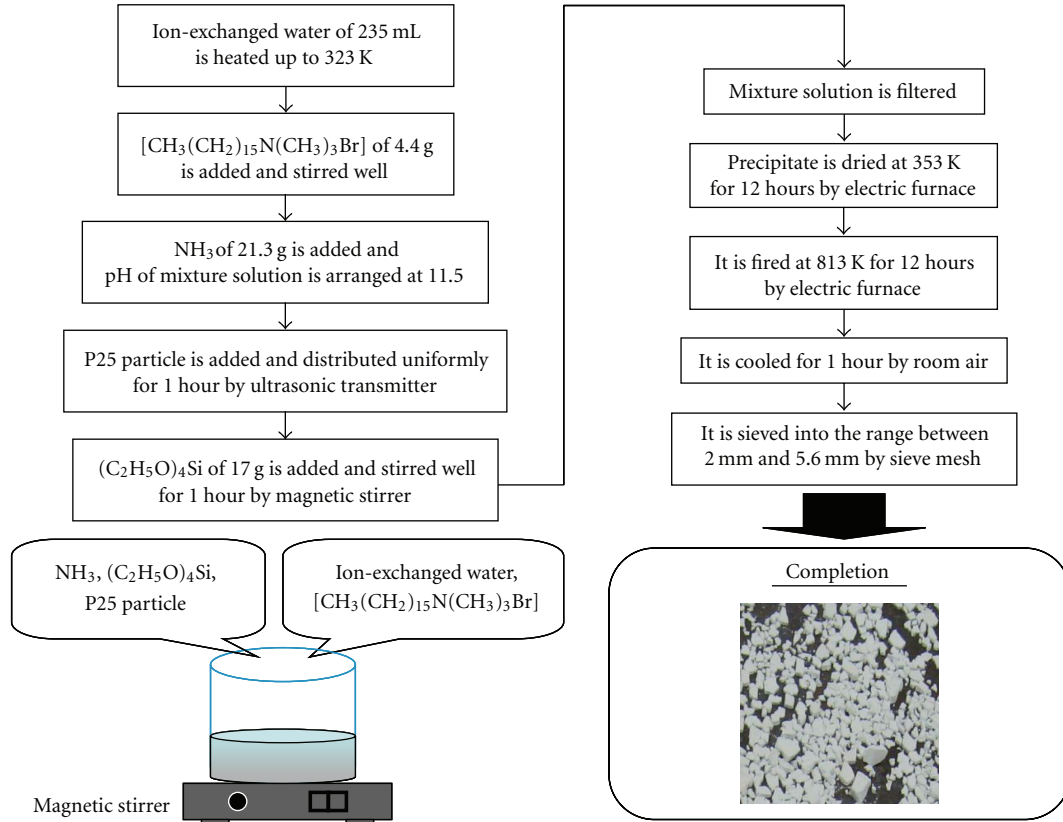


FIGURE 1: Preparation method of mesoporous silica loaded with TiO₂.

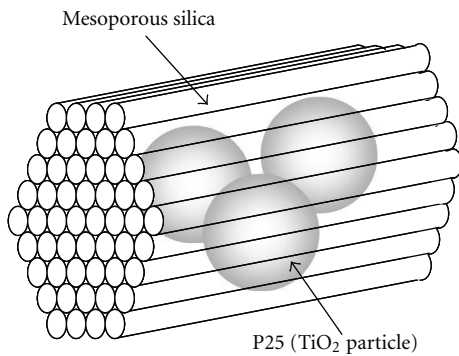
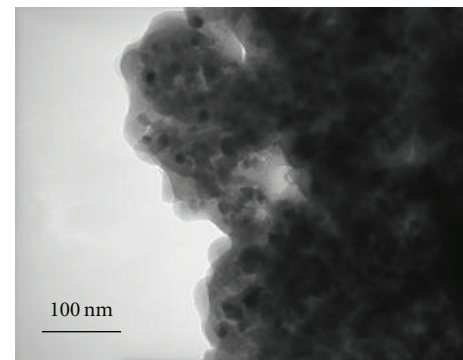


FIGURE 2: Schematic drawing of mesoporous silica loaded with TiO₂.

The selection ratio of CO oxidation is calculated by the following equation:

$$R_{\text{sel-CO}} = \frac{[\text{CO}_2] - [\text{CO}_2]_0}{([\text{CO}_2] - [\text{CO}_2]_0) + ([\text{H}_2\text{O}] - [\text{H}_2\text{O}]_0)} \times 100, \quad (14)$$

where $R_{\text{sel-CO}}$ stands for the selection ratio of CO oxidation (%), $[\text{CO}_2]$ is the concentration of CO₂ at each time (ppmV), $[\text{CO}_2]_0$ is the initial concentration of CO₂ at the beginning of the experiment (ppmV), $[\text{H}_2\text{O}]$ is the concentration of H₂O vapor at each time (ppmV), and $[\text{H}_2\text{O}]_0$ is the

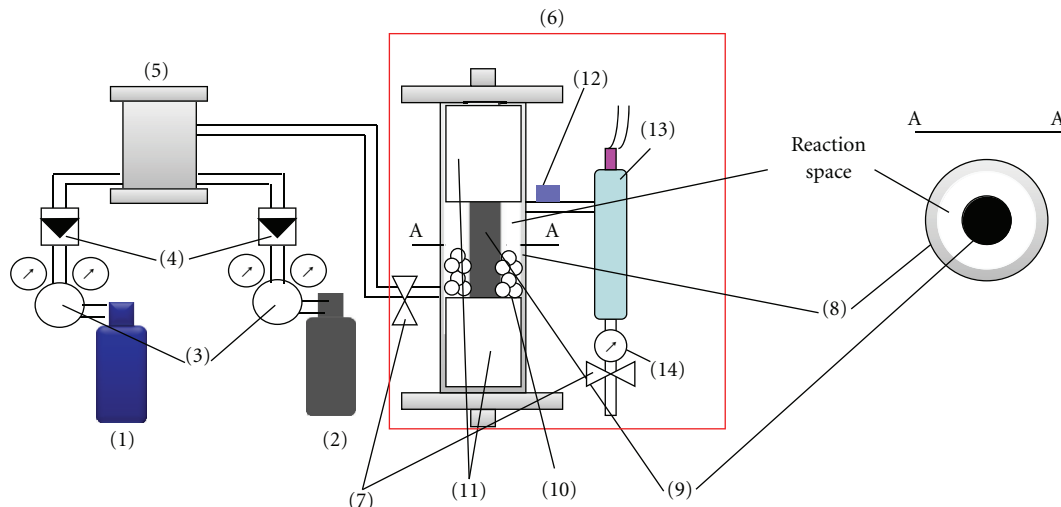


Acceleration voltage: 200 kV, × 130.000

FIGURE 3: TEM image of mesoporous silica loaded with TiO₂ particles for the ratio of loaded TiO₂ of 15 wt%.

initial concentration of H₂O vapor at the beginning of the experiment (ppmV). In this study, the selection ratio of CO oxidation means the ratio of amount of CO₂ to total oxide.

From this figure, it is known that the middle loading ratios are better compared with the lower and higher loading ratio conditions. Above all, the best selection ratio of CO oxidation is obtained for the loading ratio of TiO₂ of 20 wt%. Considering the results including $R_{\text{inc-CO}_2}$ and α , it can be said that mesoporous silica loaded with TiO₂ has



- | | | |
|---|--|-----------------------|
| (1) Premixed gas cylinder (H ₂ : 99 vol%, CO: 1 vol%) | (6) Reactor | (11) Acrylic cylinder |
| (2) O ₂ gas cylinder (99.9999 vol%) | (7) Valve | (12) Sampling tap |
| (3) Regulator | (8) Stainless pipe | (13) Dew point meter |
| (4) Mass flow controller | (9) UV lamp | (14) Pressure meter |
| (5) Gas mixing chamber | (10) TiO ₂ combined with silica | |

FIGURE 4: Experimental apparatus.

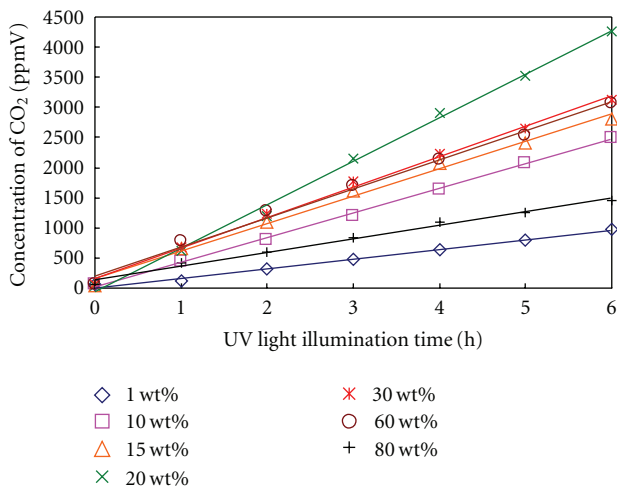


FIGURE 5: Change of concentration of CO₂ with UV light illumination time for different loading ratios of TiO₂.

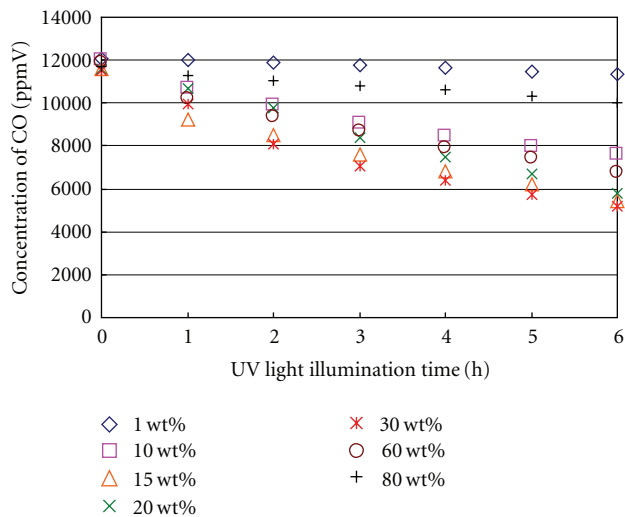


FIGURE 6: Change of concentration of CO with UV light illumination time for different loading ratios of TiO₂.

the best CO oxidation performance in the middle loading ratio, that is, around 20 wt%. According to our previous study [20], the amount of TiO₂, that is, the number of TiO₂ particle in mesoporous silica is increased with the increase in loading ratio of TiO₂. However, the adsorption performance of mesoporous silica loaded with TiO₂ is dropped with the increase in loading ratio of TiO₂ due to the pore diameter expansion and the weakening of the honeycomb shape

of mesoporous silica by increased loaded TiO₂. Therefore, it can be thought that the best match loading condition between high photocatalytic reaction performance and high adsorption performance is obtained in the middle loading ratio for the mesoporous silica loaded with TiO₂.

To evaluate the CO oxidation performance of mesoporous silica loaded with TiO₂ from diverse view points, the summation of the performance comparison factor *F* which is

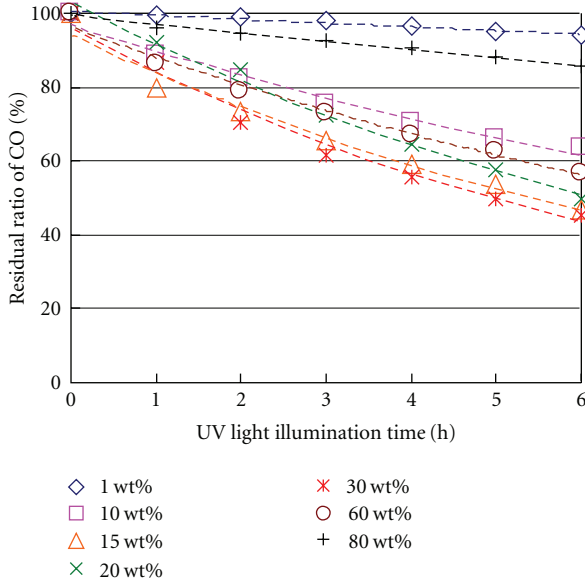


FIGURE 7: Residual ratio of CO for different loading ratio of TiO₂.

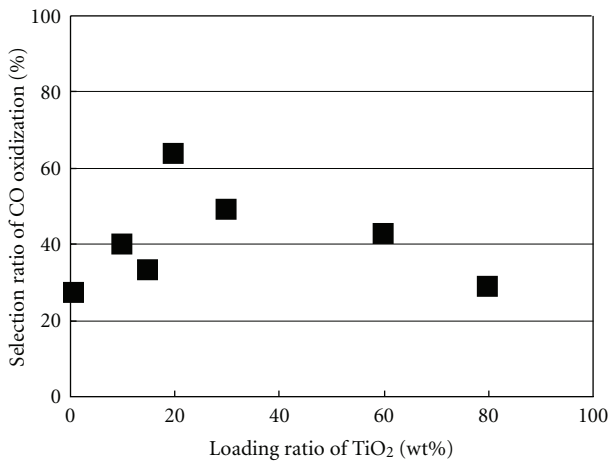


FIGURE 8: Comparison of selection ratio of CO oxidation among different loading ratio of TiO₂.

calculated by (15) is introduced:

$$F = \frac{\text{Index}_{\text{each}} - \text{Index}_{\text{ave}}}{\text{Index}_{\text{ave}}}, \quad (15)$$

where $\text{Index}_{\text{each}}$ and $\text{Index}_{\text{ave}}$ stand for the value of evaluation index on CO oxidation performance such as $R_{\text{inc-CO}_2}$, α , and $R_{\text{sel-CO}}$ under each loading ratio of TiO₂, and the average value of evaluation index on CO oxidation performance among all loading ratios of TiO₂, respectively. Here, the data after UV light illumination of 6 hours are used to calculate F for α and $R_{\text{sel-CO}}$.

Table 2 lists F and the summation of F for each loading ratio of TiO₂. From this table, it reveals that the loading ratio of TiO₂ of 20 wt% is the best loading condition. Although the middle loading ratio of TiO₂ was clarified to be suitable for CO oxidation in our previous study [20], the current

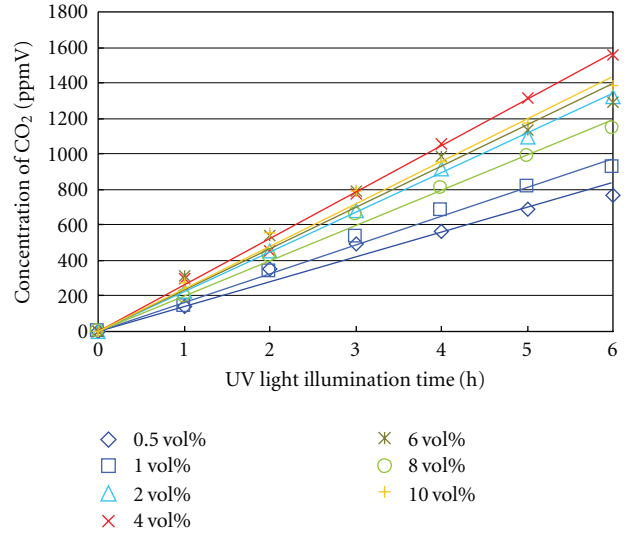


FIGURE 9: Change of concentration of CO₂ with UV light illumination time for different initial concentrations of O₂.

study confirms that the loading ratio of TiO₂ of 20 wt% is the optimum loading ratio for the promotion of the CO oxidation performance of mesoporous silica loaded with TiO₂.

3.2. Effect of Initial Ratio of O₂ to CO on CO Oxidation Performance. Figures 9 and 10 show the concentration change of CO₂ and CO with UV light illumination time for the different initial concentrations of O₂. From these figures, it can be seen that the concentration of CO for each initial concentration of O₂ is decreased with the increase in UV light illumination time, while the concentration of CO₂ is increased. According to Figure 9, $R_{\text{inc-CO}_2}$ is 139 ppmV/h, 162 ppmV/h, 223 ppmV/h, 260 ppmV/h, 232 ppmV/h, 198 ppmV/h, and 239 ppmV/h for initial concentration of O₂ of 0.5 vol%, 1 vol%, 2 vol%, 4 vol%, 6 vol%, 8 vol%, and 10 vol%, respectively. Figure 11 shows the change of residual ratio of CO with UV light illumination time for different initial concentrations of O₂. α is 1.43×10^{-2} , 2.88×10^{-2} , 4.62×10^{-2} , 5.23×10^{-2} , 4.00×10^{-2} , 3.97×10^{-2} , and 4.43×10^{-2} for initial concentration of O₂ of 0.5 vol%, 1 vol%, 2 vol%, 4 vol%, 6 vol%, 8 vol% and 10 vol%, respectively. From these results, it is confirmed that the initial concentration of O₂ exceeding the stoichiometric ratio, that is, 0.5 vol%, is necessary. In addition, $R_{\text{inc-CO}_2}$ and α are increased with the initial concentration of O₂ up to 4 vol% and decreased over 4 vol%. Since the experimental apparatus in this study is a batch type and forcible gas mixing is not carried out, it might be thought that excess amount of O₂ is necessary for O₂ to contact with CO near the surface of mesoporous silica particle loaded with TiO₂. However, the excess amount of O₂ is thought also to block the diffusions of CO to the surface and CO₂ from the surface. Consequently, there is an optimum initial concentration of O₂ existing.

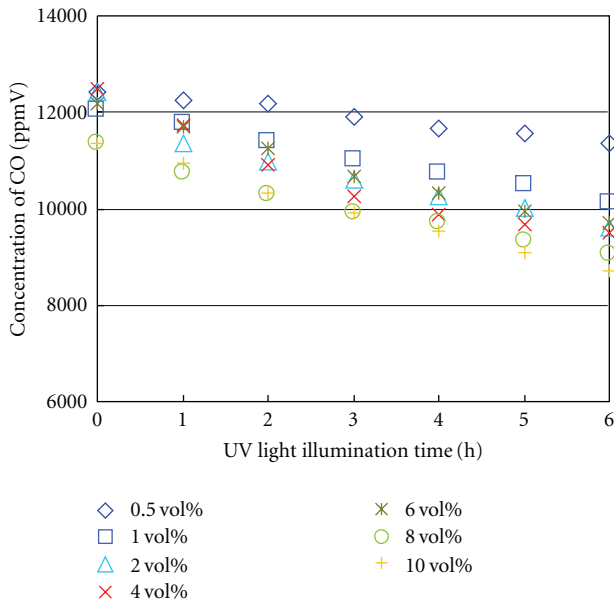
Figure 12 shows the comparison of selection ratio of CO oxidation among different initial concentrations of O₂.

TABLE 2: Comparison of F and the summation of F for each loading ratio of TiO_2 .

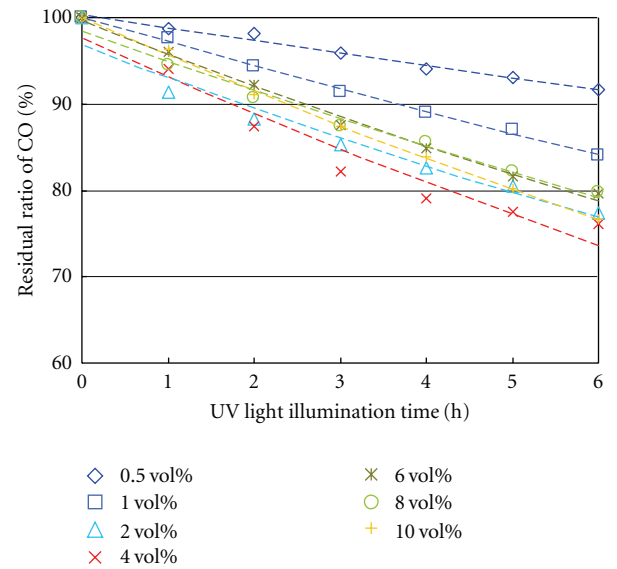
| Loading ratio of TiO_2 (wt%) | $R_{\text{inc-CO}_2}$ | F (—) | | $\sum F$ (—) |
|---------------------------------------|-----------------------|----------|---------------------|--------------|
| | | α | $R_{\text{sel-CO}}$ | |
| 1 | -0.60 | -0.87 | -0.29 | -1.76 |
| 10 | 0.027 | 0.11 | 0.045 | 0.18 |
| 15 | 0.23 | 0.75 | -0.13 | 0.85 |
| 20 | 0.76 | 0.48 | 0.67 | 1.91 |
| 30 | 0.35 | 0.89 | 0.29 | 1.53 |
| 60 | 0.31 | 0.31 | 0.11 | 0.73 |
| 80 | -0.35 | -0.66 | -0.25 | -1.26 |

TABLE 3: Comparison of F and the summation of F for each initial concentration of O_2 .

| Initial concentration of O_2 (vol%) | $R_{\text{inc-CO}_2}$ | F (—) | | $\sum F$ (—) |
|--|-----------------------|----------|---------------------|--------------|
| | | α | $R_{\text{sel-CO}}$ | |
| 0.5 | -0.33 | -0.62 | -0.37 | -1.32 |
| 1 | -0.22 | -0.24 | -0.32 | -0.78 |
| 2 | 0.074 | 0.22 | 0.23 | 0.52 |
| 4 | 0.25 | 0.38 | 0.35 | 0.98 |
| 6 | 0.12 | 0.054 | 0.29 | 0.46 |
| 8 | -0.046 | 0.046 | -0.17 | -0.17 |
| 10 | 0.15 | 0.17 | -0.013 | 0.31 |

FIGURE 10: Change of concentrations of CO with UV light illumination time for different initial concentrations of O_2 .

From this figure, it is known that the best selection ratio of CO oxidization is obtained for the initial concentration of O_2 of 4 vol%, the same as the results of $R_{\text{inc-CO}_2}$ and α as described above. With the lower initial concentration of O_2 , it seems that the CO oxidization performance is not good due to lack of gas supply to the reaction surface as mentioned above. On the other hand, CO oxidization performance declines at the higher initial concentration of O_2 . Since H_2O that is a byproduct in this reaction is

FIGURE 11: Residual ratio of CO for different initial concentrations of O_2 .

adsorbed by mesoporous silica more easily than CO , O_2 and CO_2 [24], the CO adsorption by mesoporous silica might be dropped under the higher initial concentration of O_2 . Therefore, the CO oxidization performance of mesoporous silica loaded with TiO_2 also declines. Consequently, the optimum initial concentration of O_2 is in the middle level of initial concentration of O_2 . Table 3 lists F and the summation of F for each initial concentration of O_2 . From this table, it is revealed that the initial concentration of O_2 of 4 vol%

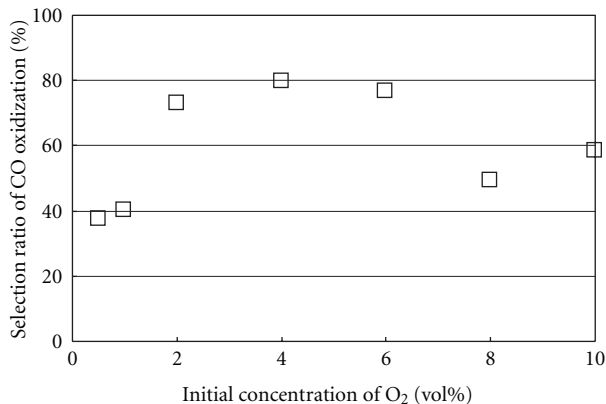


FIGURE 12: Comparison of selection ratio of CO oxidation among different initial concentrations of O₂.

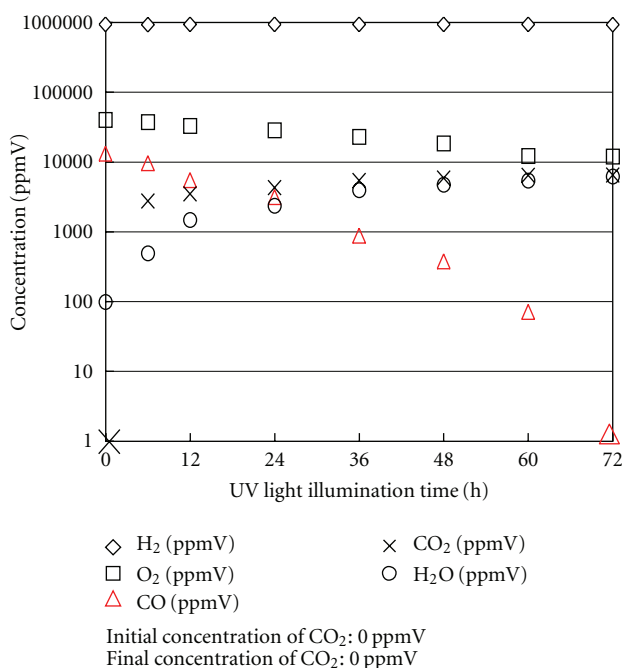


FIGURE 13: Change of each gas concentration with UV light illumination time in the long time experiment (loading ratio of TiO₂ of 20 wt%, initial concentrations of O₂ of 4 vol%).

is also the best initial concentration from diverse view points. Therefore, the optimum initial concentration of O₂ to promote the CO oxidation performance of mesoporous silica loaded with TiO₂ is decided at 4 vol%.

3.3. Evaluation on the Maximum CO Oxidation Performance of Mesoporous Silica Loaded with TiO₂. The above described results are evaluated by UV light illumination of 6 hours. To evaluate the maximum CO oxidation performance of mesoporous silica loaded with TiO₂, a longer time experiment was carried out under the optimum experimental condition as decided above.

Figure 13 shows the change of each gas concentration with UV light illumination time in the long time experiment with loading ratio of TiO₂ of 20 wt% and initial concentration of O₂ of 4 vol%. From this figure, the concentration of CO could decrease from 12000 ppmV down to 0 ppmV after UV light illumination time of 72 hours. In other words, although taking longer time, the CO was finally eliminated, which is comparable or superior to the results of the other CO oxidation processes [18, 19, 25, 26]. This proves that the proposed technology of TiO₂ combined with silica is a promising alternative CO oxidation process. To promote the CO oxidation performance of mesoporous silica loaded with TiO₂, that is, to promote the CO oxidation rate further, the investigation on the gas supply and adsorption control and UV light illumination intensity in reactor is thought to be the next subject to study.

4. Conclusions

Based on the above experimental results and discussion, the following conclusions can be drawn from this experimental study.

The optimum loading ratio of TiO₂ is around 20 wt% and the optimum initial concentration of O₂ is 4 vol% from the viewpoint of best matching of reaction rate of CO oxidation and selection ratio of CO oxidation. The best match loading condition between high photocatalytic reaction performance and high adsorption performance is in the middle loading ratio for the mesoporous silica loaded with TiO₂.

The initial concentration of O₂ in excess of the stoichiometric ratio is necessary to ensure enough gas supplied to the reaction surface. However, too much excess initial concentration of O₂ would cause the block of gas diffusion to or from the surface which undermines the CO adsorption performance and would produce too much water that was more easily adsorbed by the mesoporous silica particle loaded with TiO₂, resulting in the drop of the CO oxidation performance.

The CO of 12000 ppmV in the rich H₂ could be completely oxidized after UV light illumination time of 72 hours, which is comparable with the other CO removal methods.

References

- [1] Formenti M. and S. J. Teichner, *Catalysis*, Specialist Periodical Report, The Chemical Society, London, UK, 1978.
- [2] S. Sato, T. Kadowaki, and K. Yamaguchi, "Photo-isotope exchange between lattice oxygen and gaseous phase oxygen of oxide semiconductor—relationship with photocatalytic activity," *Catalyst*, vol. 27, no. 6, pp. 446–448, 1985.
- [3] U.S. Department of the Interior and U.S. Geological Survey, *Mineral Commodity Summaries 2006*, United States Government Printing Office, Washington, DC, USA, 2006.
- [4] J. Zhang, M. Minagawa, M. Matsuoka, H. Yamashita, and M. Anpo, "Photocatalytic decomposition of NO on Ti-HMS mesoporous zeolite catalysts," *Catalysis Letters*, vol. 66, no. 4, pp. 241–243, 2000.

- [5] H. Kominami, K. Yukishita, T. Kimura et al., "Direct solvothermal formation of nanocrystalline TiO₂ on porous SiO₂ adsorbent and photocatalytic removal of nitrogen oxides in air over TiO₂-SiO₂ composites," *Topics in Catalysis*, vol. 47, no. 3-4, pp. 155-161, 2008.
- [6] T. H. Lim and S. D. Kim, "Photocatalytic reduction of NO by CO over TiO₂/Silica gel in an annulus fluidized bed photoreactor," *Journal of the Chinese Institute of Chemical Engineers*, vol. 36, no. 1, pp. 85-89, 2005.
- [7] Y. G. Shul, H. J. Kim, S. J. Haam, and H. S. Han, "Photocatalytic characteristics of TiO₂ supported on SiO₂," *Research on Chemical Intermediates*, vol. 29, no. 7-9, pp. 849-859, 2003.
- [8] C. Cantau, T. Pigot, R. Brown et al., "Photooxidation of dimethylsulfide in the gas phase: a comparison between TiO₂-silica and photosensitizer-silica based materials," *Applied Catalysis B*, vol. 65, no. 1-2, pp. 77-85, 2006.
- [9] K. Yamaguchi, K. Inumaru, Y. Oumi, T. Sano, and S. Yamanaka, "Photocatalytic decomposition of 2-propanol in air by mechanical mixtures of TiO₂ crystalline particles and silicalite adsorbent: the complete conversion of organic molecules strongly adsorbed within zeolitic channels," *Microporous and Mesoporous Materials*, vol. 117, no. 1-2, pp. 350-355, 2009.
- [10] G. R. M. Echavia, F. Matzusawa, and N. Negishi, "Photocatalytic degradation of organophosphate and phosphoglycine pesticides using TiO₂ immobilized on silica gel," *Chemosphere*, vol. 76, no. 5, pp. 595-600, 2009.
- [11] K. Ikeue, H. Yamashita, and M. Anpo, "Photocatalytic reduction of CO₂ with H₂O on titanium oxides prepared within zeolites and mesoporous molecular sieves," *Electrochemistry*, vol. 70, no. 6, pp. 402-408, 2002.
- [12] H. Yamashita, "Photocatalytic action of highly dispersion TiO₂ prepared within pore of zeolite," in *Proceedings of the 80th Catalytic Society of Japan Meeting Abstracts (CATSJ '97)*, vol. 39, pp. 414-415, 1997.
- [13] K. I. Tanaka, Y. Moro-Oka, K. Ishigure et al., "A new catalyst for selective oxidation of CO in H₂ : part 1, activation by depositing a large amount of FeO on Pt/Al₂O₃ and Pt/CeO₂ catalysts," *Catalysis Letters*, vol. 92, no. 3-4, pp. 115-121, 2004.
- [14] M. Shou, K. I. Tanaka, K. Yoshioka, Y. Moro-Oka, and S. Nagano, "New catalyst for selective oxidation of CO in excess H₂ designing of the active catalyst having different optimum temperature," *Catalysis Today*, vol. 90, no. 3-4, pp. 255-261, 2004.
- [15] K. Tanaka and M. Shou, "Promotion effect of H₂ and H₂O on CO oxidization Reaction," in *Proceedings of the 96th Catalytic Society of Japan Meeting Abstracts (CATSJ '05)*, vol. 47, pp. 418-420, 2005.
- [16] M. Watanabe, H. Uchida, H. Igarashi, and M. Suzuki, "Pt catalyst supported on zeolite for selective oxidation of CO in reformed gases," *Chemistry Letters*, pp. 21-22, 1995.
- [17] H. Igarashi, H. Uchida, M. Suzuki, Y. Sasaki, and M. Watanabe, "Removal of carbon monoxide from hydrogen-rich fuels by selective oxidation over platinum catalyst supported on zeolite," *Applied Catalysis A*, vol. 159, no. 1-2, pp. 159-169, 1997.
- [18] T. Kamegawa, R. Takeuchi, M. Matsuoka, and M. Anpo, "Photocatalytic oxidation of CO with various oxidants by Mo oxide species highly dispersed on SiO₂ at 293 K," *Catalysis Today*, vol. 111, no. 3-4, pp. 248-253, 2006.
- [19] T. Kamegawa, M. Matsuoka, and M. Anpo, "Photocatalytic selective oxidation of CO with O₂ in the presence of H₂ over highly dispersed chromium oxide on silica under visible or solar light irradiation," *Research on Chemical Intermediates*, vol. 34, no. 4, pp. 427-434, 2008.
- [20] A. Nishimura, T. Hisada, M. Hirota, M. Kubota, and E. Hu, "Using TiO₂ photocatalyst with adsorbent to oxidize carbon monoxide in rich hydrogen," *Catalysis Today*, vol. 158, no. 3-4, pp. 296-304, 2010.
- [21] K. Inumaru, M. Murashima, T. Kasahara, and S. Yamanaka, "Enhanced photocatalytic decomposition of 4-nonylphenol by surface-organografted TiO₂: a combination of molecular selective adsorption and photocatalysis," *Applied Catalysis B*, vol. 52, no. 4, pp. 275-280, 2004.
- [22] T. Kasahara, K. Inumaru, and S. Yamanaka, "Enhanced photocatalytic decomposition of nonylphenol polyethoxylate by alkyl-grafted TiO₂-MCM-41 organic-inorganic nanostructure," *Microporous and Mesoporous Materials*, vol. 76, no. 1-3, pp. 123-130, 2004.
- [23] K. Inumaru, T. Kasahara, M. Yasui, and S. Yamanaka, "Direct nanocomposite of crystalline TiO₂ particles and mesoporous silica as a molecular selective and highly active photocatalyst," *Chemical Communications*, no. 16, pp. 2131-2133, 2005.
- [24] S. Y. Jeong, H. Jin, J. M. Lee, and D. J. Yim, "Adsorption on Ti- and Al-containing mesoporous materials prepared from fluorosilicon," *Microporous and Mesoporous Materials*, vol. 44-45, pp. 717-723, 2001.
- [25] W. Zhang, Y. Huang, J. Wang et al., "IrFeO/SiO₂-a highly active catalyst for preferential CO oxidation in H₂," *International Journal of Hydrogen Energy*, vol. 35, no. 7, pp. 3065-3071, 2010.
- [26] N. Maeda, T. Matsushima, M. Kotobuki et al., "HO₂-tolerant monolithic catalysts for preferential oxidation of carbon monoxide in the presence of hydrogen," *Applied Catalysis A*, vol. 370, no. 1-2, pp. 50-53, 2009.



Hindawi

Submit your manuscripts at
<http://www.hindawi.com>

